

1

2 **Evidence of O<sup>+</sup> ions energized by weak fast shocks in the mid-altitude cusp**

3

4 **Suping Duan<sup>1</sup>, Lou-Chuang Lee<sup>2</sup>, Lei Dai<sup>1</sup>, Chi Wang<sup>1</sup>, Chunlin Cai<sup>1</sup>**

5 <sup>1</sup> State Key Laboratory of Space Weather, National Space Science Center, Chinese Academy of  
6 Sciences, Beijing, China.

7 <sup>2</sup> Institute of Earth Sciences, Academia Sinica, Nankang, Taiwan.

8

9 Corresponding author: Suping Duan ([spduan@nssc.ac.cn](mailto:spduan@nssc.ac.cn)) and Lou-Chuang Lee  
10 ([loulee@earth.sinica.edu.tw](mailto:loulee@earth.sinica.edu.tw))

11 **Key Points:**

- 12
- Tens keV O<sup>+</sup> ions are detected by Cluster in the mid-altitude cusp.
  - O<sup>+</sup> ions are efficiently energized in the perpendicular direction to the magnetic field by  
13 weak fast shocks in the mid-altitude cusp.
  - Energetic O<sup>+</sup> ions in the mid-altitude cusp have bunch or partial ring distributions..  
14  
15  
16

**17 Abstract**

18 Oxygen ions,  $O^+$ , efficiently energized by weak fast shock in the mid-altitude cusp observed by  
19 Cluster on 7 November 2004 are investigated in this paper. An interplanetary fast shock hitting  
20 Earth magnetosphere was observed by Geotail spacecraft at 1825 UT with a sharply increase in  
21 the solar wind dynamic pressure from 3nPa to 11nPa. There are significant fluctuations of solar  
22 wind dynamic pressure in the interval of 1930 UT to 2000 UT during this long time fast shock  
23 compressing Earth magnetosphere. During this pressure disturbance intervals Cluster 4 was  
24 located in the mid-altitude cusp, (0.43, -3.25, 3.07)  $R_{E\_GSE}$ . CODIF/Cluster 4 instrument detected  
25  $O^+$  ions with tens keV energy energized by the weak fast shock with Mach number  $M_A \sim 1.2$  in  
26 the perpendicular direction. Those energetic  $O^+$  ions associated with the weak fast shock have  
27 bunch or partial ring distributions in the mid-altitude cusp. Our observation results put forward  
28 confident evidences on the weak fast shock efficiently energizing heavy ions, especially,  $O^+$  ions  
29 in the cusp.

**30 Plain Language Summary**

31 Singly charged oxygen ions,  $O^+$ , origin from the ionosphere with very low energy have low  
32 outflow speed. Usually, the energy of  $O^+$  ions in the mid-altitude cusp is as low as  $\sim 300$  eV. An  
33 energization mechanism for the low energy  $O^+$  ions is needed for their outflow. The broadband  
34 low frequency waves (BBLFW) and ambipolar electric fields are the main mechanisms for  $O^+$   
35 ions outflow. But the mechanism energizing  $O^+$  ions to tens keV still remains to be understood.  
36 In this report we present a new efficient mechanism for  $O^+$  ions energizations. The weak fast  
37 shocks in the magnetosphere can energize  $O^+$  ions to tens keV in the mid-altitude cusp.

## 38 **1 Introduction**

39 Oxygen ions,  $O^+$ , origin from the ionosphere, play a significant role in the magnetospheric  
40 dynamics during intense geomagnetic storms and substorms [e.g., Daglis, 2006; Duan et al.,  
41 2017; 2019; Fu et al., 2001; Kistler et al.,2016; Zeng et al., 2020]. The energy density of  
42 energetic  $O^+$  ions can be a dominant component with larger than 50% of ring current during  
43 intense storms [e.g., Daglis and Axford, 1996; Fu et al., 2001]. The cusp is one of major source  
44 regions of  $O^+$  ions which are distributing in the magnetospheric active regions, such as, plasma  
45 sheet and ring current [e.g., Kistler et al.,2016; Liao et al.2010; Yau et al.,1997; Yu and  
46 Ridley.,2013]. Previous studies reported that the energy of  $O^+$  ions upflowing from the  
47 ionosphere was very low,  $\sim$  eV [e.g., Yau et al., 2007]. They can be energized to higher energy  
48 with escaping velocity and outflow into the higher altitude polar region [Andre et al., 1990; Yau  
49 et al., 2007].  $O^+$  ions can be transversely energized to tens and hundred eV in the mid-altitude  
50 cusp by the broadband low frequency waves (BBLFW) [e.g., Andre et al., 1990; Chang et al.,  
51 1986; Yau et al., 2007; Bouhram et al., 2004; Slapak et al.,2011].

52  
53 Duan et al. [2019] reported that there were counter-stream  $O^+$  ions with energy  $\sim$ 10s keV in  
54 sequential flux ropes in the high altitude cusp. They proposed that the mid-altitude cusp was one  
55 source region of these energetic  $O^+$  ions in the high altitude cusp. While,  $O^+$  ions in the mid-  
56 altitude cusp are usually with energy  $\sim$ 300 eV [e.g., Yau et al., 2007; Bouhram et al., 2004].  $O^+$   
57 ions with energy  $\sim$ 10s keV in the mid-altitude cusp are rarely reported. The energization  
58 mechanism for these outflow  $O^+$  ions with high energy in the mid-altitude cusp still remains to  
59 be solved.

60

61 Previous research work indicates that the weak fast perpendicular shock can efficiently  
62 accelerate ions, especially, heavy ions [e.g., Lee et al., 1986; Lee et al., 1987; Lee and Lee,  
63 2016]. Simulation results of significant ion heating by quasi-perpendicular shock were first  
64 reported by Lee et al. [1987]. The accelerated ions show a ring or bunch velocity distribution in  
65 the downstream region of weak fast shocks [e.g., Lee et al., 1987; Lee and Lee, 2016]. Lee and  
66 Wu [2000] reported that the weak fast shock with  $1.1 < M_A < 1.5$  can accelerate heavy ions, such  
67 as  $O^{5+}$ , to high speed  $\sim 460$  km/s in the solar wind. Lee and Lee [2016] reported that the weak fast  
68 shocks in the magnetosphere were driven by the solar wind dynamic pressure enhancements or  
69 fast shocks in the solar wind through interaction with bow shock and magnetopause.

70

71 The mechanisms for  $O^+$  ions energized up to 10s keV in the mid-altitude cusp is an interesting  
72 subject. This energization process still remains to be understood. Using conjunction observations  
73 of Geotail spacecraft in the dayside interplanetary space and Cluster in the mid-altitude cusp 7 on  
74 November 2004, demonstrate that the  $O^+$  ions are energized from hundred eV to tens keV in the  
75 mid-altitude cusp by weak fast shocks associated with solar wind dynamic pressure increase. The  
76 detailed analysis is presented in sections 2 and 3. Discussion and summary are presented in  
77 section 4. The GSE coordinates are adopted in our paper.

## 78 **2 Conjunction observations of weak fast shocks in the mid-altitude cusp**

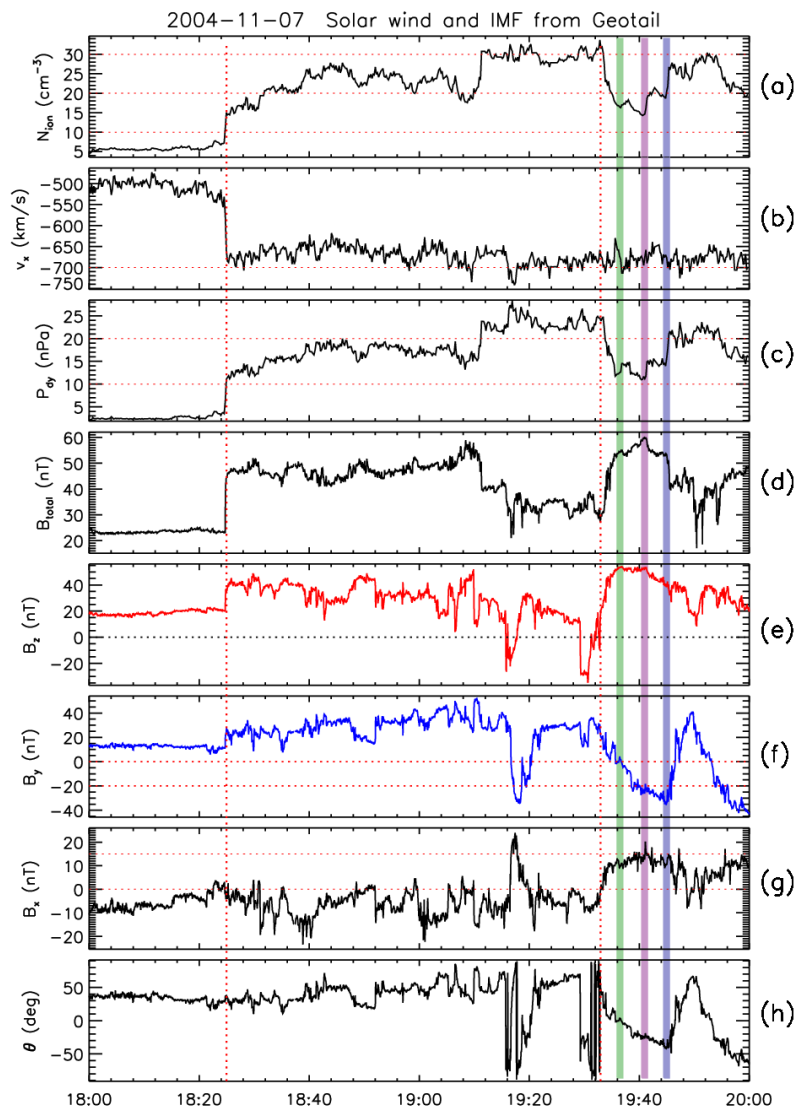
79 The solar wind density and velocity and interplanetary magnetic field (IMF) during an  
80 interplanetary shock on 7 November 2004 detected by Geotail spacecraft located around (19.0,  
81 12.0,-5.0)  $R_E$  are presented in Figure 1. The solar wind number density and velocity are both  
82 very high, as shown in Figure 1a and Figure 1b, respectively.  $N_{ion}$  is in the range from  $10 \text{ cm}^{-3}$  to  
83  $30 \text{ cm}^{-3}$ . The solar wind speed is around  $\sim 650$  km/s and remained for a long time interval  $\sim 2$

84 hours. The solar wind dynamic pressure increased sharply from 5nPa to 10 nPa at 1827 UT as  
85 marked by the first vertical red dotted line in Figure 1c. At the same time, the magnetic field  
86 magnitude also increase from 23nT to 45nT as presented in Figure 1d. The  $B_z$  and  $B_y$   
87 components both increase significantly, as shown in Figure 1e and 1f, respectively. The  $B_x$   
88 component does not change clearly as presented in Figure 1g. The dominant component  $B_z$   
89 increases from 20 nT to 38 nT as marked by the first vertical dotted line in Figure 1e. The solar  
90 wind dynamic pressure and magnetic field increase simultaneously, indicating that a  
91 perpendicular shock is detected. We calculate the shock normal angle  $\sim 80$  degree and the Alfvén  
92 Mach number of this shock,  $M_A \sim 1.9$ , as the  $B_z$  component being tangent to the shock plane. The  
93  $B_z$  and  $B_y$  component both retain mainly positive value for about 1 hour interval as shown in  
94 Figure 1e and 1f. These plasma and electromagnetic field characteristics indicate that the fast  
95 shock will compress the magnetosphere after 1827 UT. The high solar wind dynamic pressure  
96 maintained a large value for more than 1.5 hour, as shown in Figure 1c. It means that this fast  
97 shock lasted for a long time intervals. There are several significant fluctuations in the solar wind  
98 number density and magnetic field. At 1933UT, the solar wind dynamic pressure decrease  
99 sharply, from 25 nPa to 12 nPa, as marked by the second red vertical dotted line in Figure 1c.  
100 After this dynamic pressure decreased, the solar wind dynamic pressure increased significantly at  
101 1937UT, 1941UT, 1945UT, as marked by three color shaded regions, as green, pink and blue in  
102 Figure 1c, respectively. Accompanied with these dynamic pressure enhancements the magnetic  
103 field  $B_t$  increases slightly, as shown in Figure 1d. These are significant signatures for weak fast  
104 shocks. During these weak fast shock the  $B_z$  component is dominant with large positive value  
105  $\sim 40$  nT, as displayed in Figure 1e. The  $B_y$  component is dominantly negative around  $\sim -20$  nT, as  
106 presented in Figure 1f. When these fast shocks passed through Earth magnetosphere their velocity

107 slows down. The Mach number  $M_A$  is around 1.2. As mentioned by Zong et al. [2009] and Lee  
108 and Lee [2016], this weak fast shock played a significant role in the magnetosphere dynamic.  
109 Figure 2 shows the corresponding signatures of these weak fast shocks in the mid-altitude cusp  
110 observed by Cluster during 1930UT to 2000 UT.

111

112



113

114 **Figure 1.** Solar wind plasma and IMF during a fast shock detected by Geotail on 7 November  
 115 2004 are displayed. From top to bottom, panels are (a) solar wind ions number density,  $N_{\text{ion}}$ , ( $\text{cm}^{-3}$ ),  
 116  $^3$ ), (b) the x component velocity of ions,  $v_x$ , (km/s), (c) solar wind dynamic pressure,  $P_{\text{dy}}$ , (nPa),  
 117 (d) the total magnitude of IMF,  $B_t$ , (nT), (e) IMF  $B_z$ , (f) IMF  $B_y$ , (g) IMF  $B_x$ , (h) the IMF clock  
 118 angle,  $\theta = \arctan(B_y/B_z)$ , respectively.

119

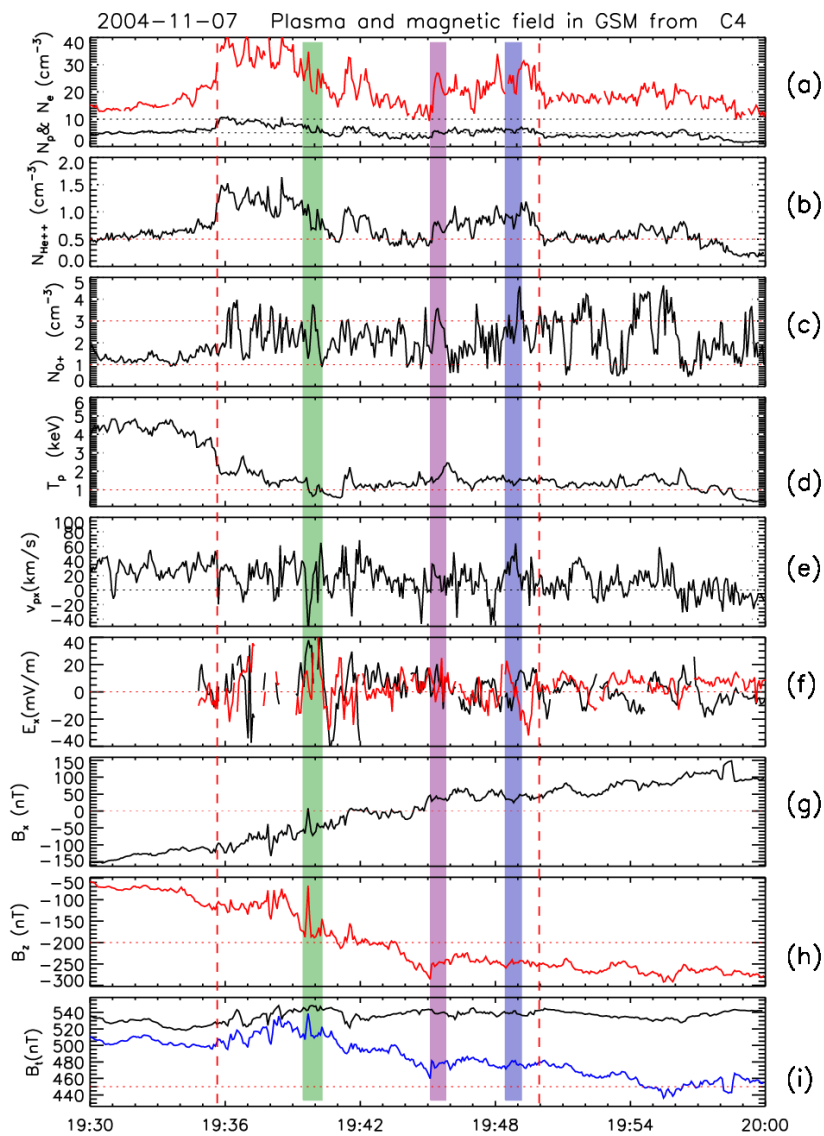
120 As the reaction of the solar wind dynamic pressure decreased significantly from 25nPa to 10nPa  
121 at 1933UT in Figure 1c, the Earth magnetosphere expanded outward. Thus Cluster C4 located at  
122 the northern hemisphere (0.55,-3.33, 2.90)  $R_E$  encountered the cusp. The high number density of  
123 ions and electrons were detected by Cluster C4; both increased sharply at 193530UT, as marked  
124 by the first red vertical dashed line in Figure 2a. Between two red vertical dashed lines, the  
125 number density of  $He^{++}$  is high, larger than  $0.5 \text{ cm}^{-3}$  as shown in Figure 2b. The x component of  
126 proton velocity is low with 50km/s fluctuations as presented in Figure 2e. The magnetic field has  
127 significant fluctuations in three components as shown in the bottom three panels, Figures 2g to  
128 2i. These plasma and magnetic field features are consistent with the characteristics in the mid-  
129 altitude cusp [e.g., Guo et al., 2008; Duan et al., 2006]. With  $\sim 3$  min lag for time shift from  
130 Geotail location to Cluster/SC4 location, the weak fast shocks play significant role in  $O^+$  ions  
131 energization in the mid-altitude cusp. Three color shade regions in Figure 2 are corresponding  
132 three weak fast shocks observed by Geotail in dayside solar wind space with one-to-one  
133 relationship, respectively. As shown in Figures 2a to 2c and Figures 2g to 2i, in these three shade  
134 regions, electrons and ions density and the magnetic field significantly increase. The  $B_y$  is the  
135 dominant component of the magnetic field during these three intervals. For simplicity we assume  
136 the y component as the field tangential to the shock normal plane. Using the method reported by  
137 Lee and Lee [2016], we calculate the upstream angle between the background magnetic field and  
138 shock normal  $\theta_{BN} = 54$  degree, and the Alfvén Mach number  $M_A = 1.11$ . Within these regions, the  
139 number density of  $O^+$  ions increases significantly, from  $2 \text{ cm}^{-3}$  to  $4 \text{ cm}^{-3}$ , as shown in Figure 2c.  
140 The electric field is very large,  $\sim 10$ s mV/m, and especially, in the first shade regions, the  $E_x$   
141 component approaches to 40 mV/m as presented in Figure 2f. These weak fast shocks are  
142 accompanied with a significant large electric field  $E_x$  in the perpendicular direction to the

143 magnetic field and they are associated with a significant increase of O<sup>+</sup> ions number density in  
144 the mid-altitude cusp.

145

146

147



148

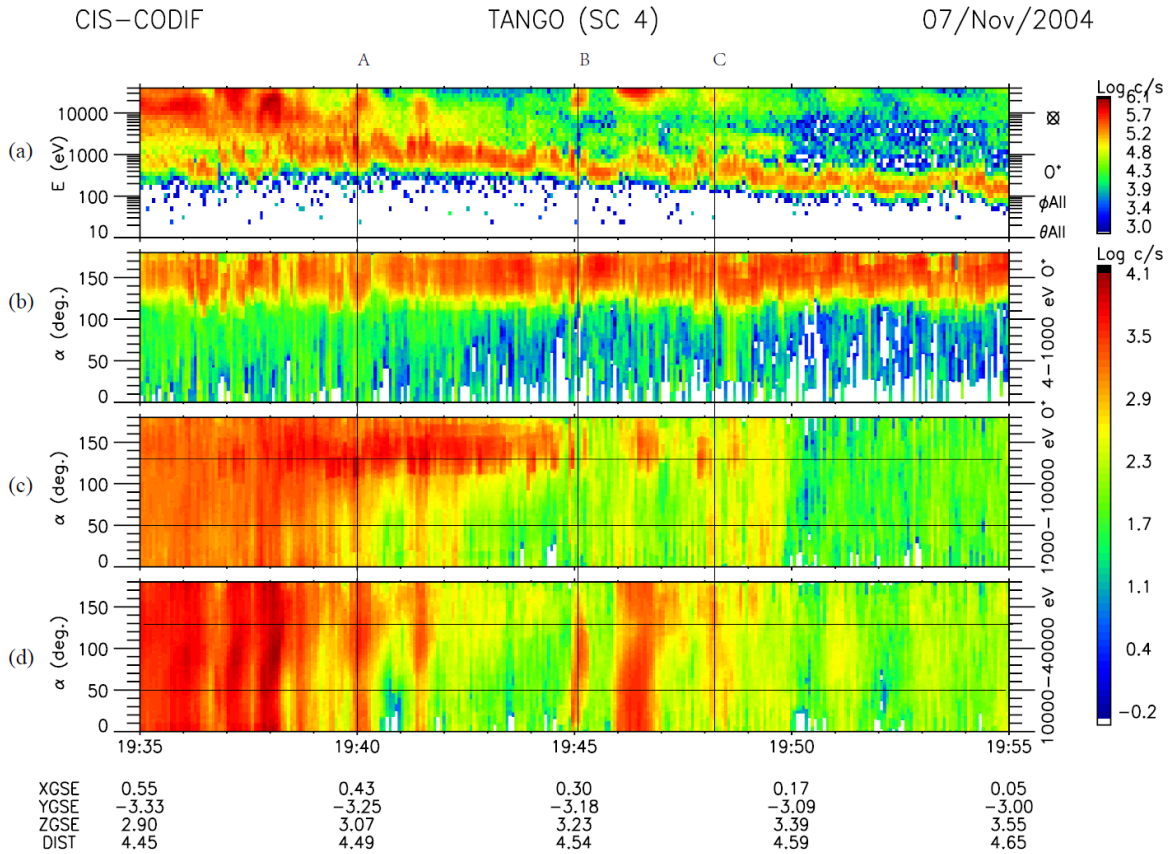
149 **Figure 2.** Plasma and electromagnetic field in the mid-altitude cusp observed by Cluster/SC4 on  
 150 7 November 2004. From top to bottom, the panels are (a) proton and electron number density,  $N_p$   
 151 (black),  $N_e$  (red), ( $\text{cm}^{-3}$ ), (b) Helium number density,  $N_{\text{He}^{++}}$ , ( $\text{cm}^{-3}$ ), (c) O+ ion number density,  
 152  $N_{\text{O}^+}$ , ( $\text{cm}^{-3}$ ), (d) Proton temperature  $T_p$  (keV), (e) X component of proton velocity,  $v_{px}$ , (km/s),  
 153 (f) the X and Z components of the electric field,  $E_x$  (black),  $E_z$  (red) (mV/m), (g)  $B_x$  (nT), (h)  $B_z$ ,  
 154 (i)  $B_t$  (black) and  $B_y$  (blue), respectively.

155

### 156 **3 Evidence of O<sup>+</sup> energized by weak fast shocks in the mid-altitude cusp**

157 The energy flux and pitch angle distributions of O<sup>+</sup> ions obtained from CODIF/CIS instrument  
158 [Reme et al., 2001] onboard Cluster/SC4 in the mid-altitude cusp in the intervals from 1935UT  
159 to 1955UT on 7 November 2004 are presented in Figure 3. During the intervals from 1936 UT to  
160 1950 UT Cluster C4 is located in the northward hemisphere mid-altitude cusp. Thus, the O<sup>+</sup> ions  
161 pitch angle is within a large degree range, from 135 degree to 180 degree, indicating that these  
162 oxygen ions are outflow from the cusp region, as shown in Figure 3b. These O<sup>+</sup> ions are mainly  
163 with low energy less than 1keV. But the pitch angle of O<sup>+</sup> ions with higher energy larger than10  
164 keV shows significant flux increase around ~90 degree, i.e., in the range of 45 degree to 135  
165 degree, especially, at 1940 UT, 1945 UT, and 194830UT as marked by three black vertical lines  
166 in Figure 3d, respectively. These three times are all within the time intervals corresponding to  
167 three color shade regions assigned as green, pink and blue in Figure 2, respectively. The pitch  
168 angle around 90 degree means energetic O<sup>+</sup> ions are distributed dominantly in quasi-  
169 perpendicular direction to the magnetic field. In order to show more features of these high energy  
170 O<sup>+</sup> ions, we will present the detailed oxygen ions velocity distributions in the vicinity of these  
171 three times.

172



173

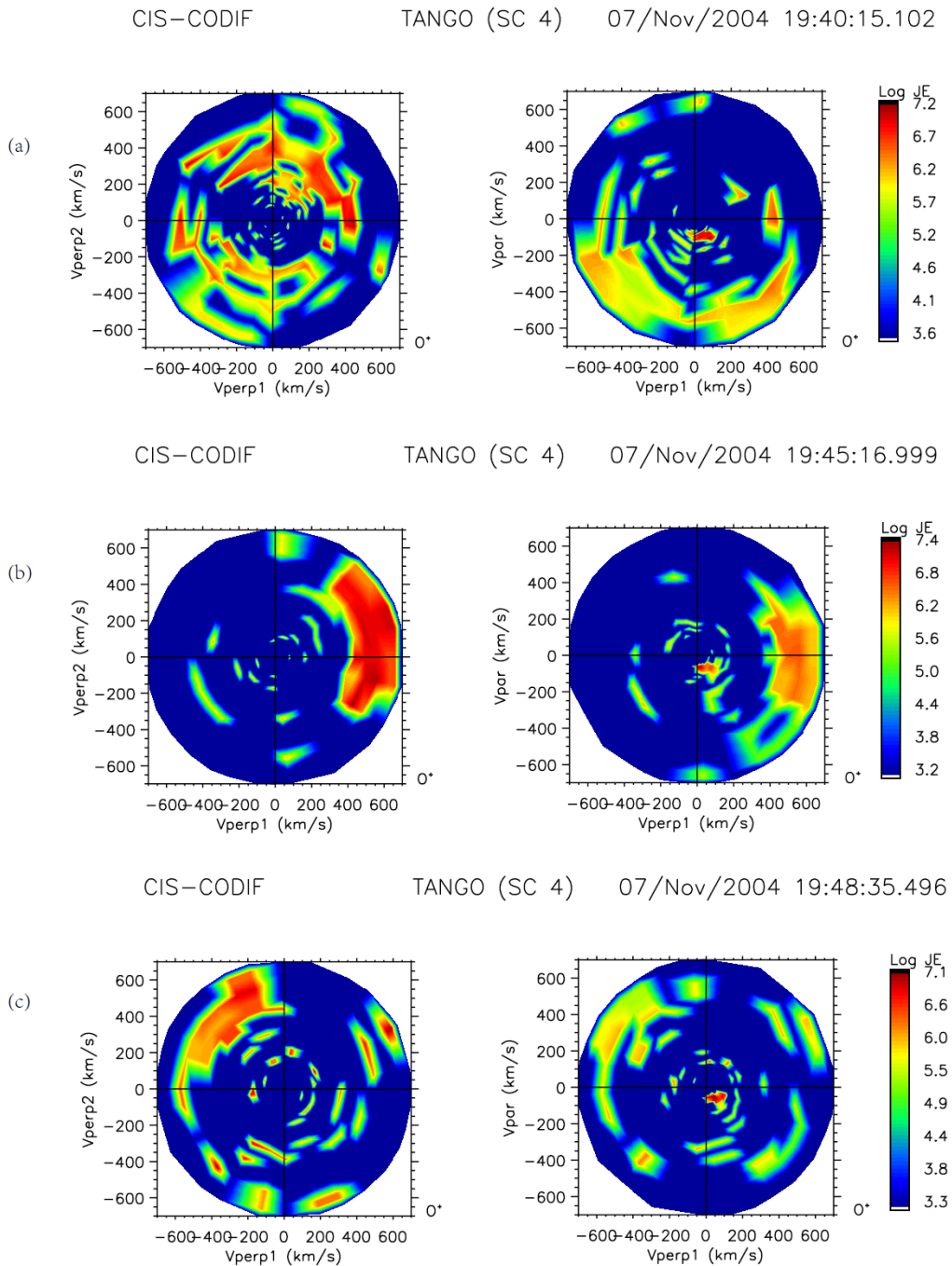
174

175 **Figure 3.** Energetic oxygen ions energy flux and pitch angle distributions observed in the mid-  
 176 altitude cusp regime. (a)  $O^+$  ions energy flux, (b) to (d) the pitch angle of  $O^+$  ions with energy  
 177 range (4 to 1000eV), (1keV-10keV) and (10keV-40keV), respectively. The vertical lines  
 178 assigned as A,B,C marked the time of  $O^+$  ions energy flux sharply enhancement with quasi-  
 179 perpendicular pitch angle in the high energy range around 1940 UT, 1945UT, and 194830UT,  
 180 respectively, which correspond to the three shaded color regions in Figure 2.

181

182 Figure 4 presents the  $O^+$  ions velocity distributions at 194015 UT, 194516 UT, and 194835 UT,  
 183 respectively. These three times are marked by three black vertical lines assigned as ‘A’, ‘B’, and

184 'C' in Figure 3. Energetic  $O^+$  ions with tens keV energy at these three times are dominant in the  
185 quasi-perpendicular direction with pitch angle in the range 45 degree to 135 degree, as shown in  
186 Figure 3d. At these three times, energetic  $O^+$  ions velocity distributions, displayed in Figure 4a to  
187 4c, respectively, have bunch or partial ring distributions.  $O^+$  ions are energized by the weak fast  
188 shocks with intense perpendicular electric field ( $E_x$ ), as shown in Figure 2f with three color shade  
189 regions. They are all associated with the solar wind dynamic pressure increases assigned as three  
190 shaded color regions in Figure 1c. These observational energetic  $O^+$  ions having bunch or partial  
191 ring distributions are consistent with the simulation results reported by Lee et al [1987]. They  
192 proposed that ions can be energized by the weak fast shock in the perpendicular directions to the  
193 background magnetic field. Our observation results present that  $O^+$  ions accelerations are  
194 associated with the significant intense electric field in the weak fast shock structures. As shown  
195 in Figure 2f the electric fields have significant enhancements with large-amplitude fluctuations,  
196 the maximum value is  $E_x \sim 40$  mV/m.



197

198 **Figure 4.** Two-dimensional cuts of the three-dimensional  $O^+$  ions velocity distributions obtained  
 199 by CODIF/C4 in the mid-altitude cusp at 194015 UT, 194516 UT, and 194835UT, respectively.

200

## 201 **4 Discussion and Summary**

202 As mentioned above when Cluster/SC4 crossing the mid-altitude cusp in dawnside during the  
203 intervals from 1935 UT to 1950 UT on 7 November 2004, the IMF  $B_z$  component is positive with  
204 a large value from 20 nT to 50 nT. The IMF  $B_y$  component is negative with  $\sim -20$  nT. Thus, this  
205 large positive  $B_z$  component implies that there is no effect of dayside magnetic reconnection on  
206 the cusp during this period. On the other hand, under this IMF condition the cusp location shifts  
207 to the dawnward. Pitout et al [2006] reported that during the northward IMF the location of the  
208 cusp depending primarily upon the solar dynamic pressure and the Y-component of IMF. Figure  
209 1c shows that the solar wind dynamic pressure has three step enhancements from 10 nPa to 23  
210 nPa at 1937 UT, 1941 UT and 1945 UT. Under this large solar wind dynamic pressure, the cusp  
211 spatial scale can expand to a larger size. Thus the solar wind dynamic pressure dominantly  
212 controls the cusp location during this interval.

213  
214 Lee and Lee [2016] proposed that weak fast shocks can be driven by the solar wind dynamic  
215 pressure enhancements. Figure 3a displays significant enhancements of tens keV  $O^+$  ions energy  
216 flux spectrum at 1940 UT, 1945 UT and 1948 UT. These enhancements are associated with the  
217 solar wind dynamic pressure increases in Figure 1c at 1937 UT, 1941 UT and 1945 UT,  
218 respectively. The corresponding energetic  $O^+$  ions pitch angle distributions as shown in Figure  
219 3d have significant quasi-perpendicular signatures. These associated observations imply that the  
220 three weak fast shocks accelerated  $O^+$  ions in the perpendicular direction to the magnetic field.

221  
222 A thin ramp with spatial scale smaller than ion inertial length is a significant property for a  
223 quasi-perpendicular shock [e.g., Leroy et al., 1982; Lee et al., 1986]. The weak fast shocks are

224 accompanied with a significant perpendicular electric field as addressed by Lee and Wu [1990],  
225 especially, through the shock ramps. Figure 2f shows that there really are significant  
226 perpendicular electric fields,  $E_x$ , associated with these weak fast shocks detected by Cluster/SC4  
227 in the mid-altitude cusp. Within shock ramp the perpendicular electric field with large amplitude  
228 can efficiently accelerate  $O^+$  ions. As shown in three color shade regions in Figure 2f, the X  
229 component of the electric field has a large amplitude,  $E_x \sim 40\text{mV/m}$ ,  $10\text{mV/m}$  and  $20\text{mV/m}$ ,  
230 respectively. These three large perpendicular electric fields in the shock ramp with spatial scale  
231 100km are corresponding to quasi-perpendicular pitch angle of energetic  $O^+$  ions with energy  
232 tens keV as marked by three vertical black lines, respectively, in Figure 3a and 3d.

233

234 Lee and Wu [2000] proposed that the weak fast shock could energize heavy ions in the direction  
235 perpendicular to background magnetic field leading to a bunch or partial ring velocity  
236 distribution. Our investigations on these energized  $O^+$  ions velocity distributions at three time  
237 194015UT, 194516UT and 194835UT display bunch or partial ring distribution as shown in  
238 Figure 4a, 4b and 4c, respectively. It demonstrates that our observation results provide confident  
239 evidences for previous theory and simulation results [e.g., Lee et al., 1986; Lee et al., 1987; Lee  
240 and Wu 2000; Lin et al., 2004].

241

242 Tens of keV  $O^+$  ions in the mid-altitude cusp associated with weak fast shocks are observed by  
243 Cluster/SC4. These energetic  $O^+$  ions can outflow into the high-altitude cusp. Duan et al [2019]  
244 reported that energetic  $O^+$  ions with energy  $\sim$  tens keV in the high-altitude cusp have counter-  
245 streaming distributions. They suggested that the mid-altitude cusp was one source region of these  
246 energetic  $O^+$  ions. Our studies provide confident evidences that  $O^+$  ions can be efficiently

247 energized by weak fast shock to tens keV in the mid-altitude cusp. These energetic  $O^+$  ions may  
248 flow outward into high-altitude cusp.

249

250 Based on conjunction observations between Geotail in the solar wind and Cluster in the mid-  
251 altitude cusp on 7 November 2004, we propose a new mechanism for  $O^+$  ions, which are  
252 efficiently energized by weak fast shock to tens keV in the mid-altitude cusp. These energetic  $O^+$   
253 ions present bunch or partial ring distribution in the mid-altitude cusp. Our observations results  
254 provide some confident evidences that the weak fast shock can efficiently energize heavy ions,  
255 especially,  $O^+$  ions in the cusp region.

## 256 **Acknowledgments**

257 We acknowledge the use of data from the ESA Cluster Science Archive  
258 (<http://www.cosmos.esa.int/web/csa>). We thank the FGM, CIS, EFW and PEACE instrument  
259 teams. Geotail magnetic field (plasma) data were provided by T.Nagai (Y. Saito) through  
260 DARTS at Institute of Space and Astronautical Science, JAXA in Japan  
261 (<https://darts.isas.jaxa.jp/stp/geotail/>). This work is supported by the National Natural Science  
262 Foundation of China grants 41874196,41731070, 41674167,41574161 and 41574159; the  
263 Strategic Pioneer Program on Space Science, Chinese Academy of Sciences, grants  
264 XDA15017000, XDA15052500, XDA15350201 and XDA15011401; the NSSC Research Fund  
265 for Key Development Directions and in part by the Specialized Research Fund for State Key  
266 Laboratories.

267

268 **References**

- 269 Andre, M., Crew, G. B., Peterson, W. K., Persoon, A. M., & Pollock, C. J. (1990). Ion heating by  
270 broadband low-frequency waves in the cusp/cleft. *Journal of Geophysical Research*, 95,  
271 20,809–20,823. <https://doi.org/10.1029/JA095iA12p20809>
- 272 Bouhram, M., Klecker, B., Miyake, W., Rème, H., Sauvaud, J.-A., Malingre, M., Kistler, L.,  
273 and Blagau, A. (2004). On the altitude dependence of transversely heated O<sup>+</sup> distributions in  
274 the cusp/cleft, *Ann. Geophys.*, 22, 1787–1798, doi:10.5194/angeo-22-1787-2004.
- 275 Chang, T., G. B. Crew, N. Hershkowitz, J. R. Jasperse, J. M. Retterer, and J. D. Winningham  
276 (1986), Transverse acceleration of oxygen ions by electromagnetic ion cyclotron resonance  
277 with broad band left-hand polarized waves, *Geophys. Res. Lett.*, 13(7), 636–639, doi:10.1029/  
278 GL013i007p00636.
- 279 Daglis, I. A., & Axford, W. I. (1996). Fast ionospheric response to enhanced activity in  
280 geospace: Ion feeding of the inner magnetotail. *Journal of Geophysical Research*, 101(A3),  
281 5047–5065. <https://doi.org/10.1029/95JA02592>
- 282 Daglis, I. A. (2006), Ring current dynamics, *Space Sci. Rev.*, 124(1), 183–202,  
283 doi:10.1007/s11214-006-9104-z.
- 284 Duan, S.-P., et al. (2006), Analysis of the interaction between low-frequency waves and ions in  
285 the high-altitude cusp region observed by Satellite Cluster, *Chin. Phys. Lett.*, 23(5), 1351–  
286 1354.
- 287 Duan, S., Dai, L., Wang, C., He, Z., Cai, C., Zhang, Y. C., ... Khotyaintsev, Y. V. (2017).  
288 Oxygen ions O<sup>+</sup> energized by kinetic Alfvén eigenmode during dipolarizations of intense  
289 substorms. *Journal of Geophysical Research: Space Physics*, 122. <https://doi.org/10.1002/>  
290 2017JA024418

- 291 Duan, S., Dai, L., Wang, C., Cai, C., He, Z., Zhang, Y., et al (2019). Conjunction observations of  
292 energetic oxygen ions O<sup>+</sup> accumulated in the sequential flux ropes in the high-altitude cusp.  
293 *Journal of Geophysical Research: Space Physics*, 124 . <https://doi.org/10.1029/2019JA026989>
- 294 Fu, S. Y., Q. G. Zong, T. A. Fritz, Z. Y. Pu, and B. Wilken, Composition signatures in ion  
295 injections and its dependence on geomagnetic conditions, *J. Geophys. Res.*, 107(A10), 1299,  
296 doi:10.1029/2001JA002006, 2002.
- 297 GUO Jian-Guang, SHI Jian-Kui, ZHANG Tie-Long, LIU Zhen-Xing (2008), Interhemispheric  
298 comparison of dipole tilt angle effects on latitude of mid-altitude cusp, *Chinese Physics*  
299 *Letter*, 25(5),1916-1918.
- 300 Kistler, L. M., et al. (2016), The source of O<sup>+</sup> in the storm time ring current, *J. Geophys. Res.*  
301 *Space Physics*, 121, doi:10.1002/2015JA022204.
- 302 Lee, K. H., and L. C. Lee (2016), Generation of He<sup>+</sup> and O<sup>+</sup> EMIC waves by the bunch  
303 distribution of O<sup>+</sup> ions associated with fast magnetosonic shocks in the magnetosphere,  
304 *Geophys. Res. Lett.*, 43, 9406–9414, doi:10.1002/ 2016GL070465.
- 305 Lee, L. C., and B. H. Wu (2000), Heating and acceleration of protons and minor ions by fast  
306 shocks in the solar corona, *Astrophys. J.*, 535, 1014.
- 307 Lee, L. C., C. S. Wu, and X. W. Hu (1986), Increase of ion kinetic temperature across a  
308 collisionless shock: 1. A new mechanism, *Geophys. Res. Lett.*, 13, 209.
- 309 Lee, L. C., M. E. Mandt, and C. S. Wu (1987), Increase of ion kinetic temperature across a  
310 collisionless shock: 2. A simulation study, *J. Geophys. Res.*, 92, 13,438.
- 311 Leroy, M. M., D. Winske, C. C. Goodrich, C. S. Wu, and K. Papadopoulos, The structure of  
312 perpendicular bow shocks, *J. Geophys. Res.*, 87, 5081-5094, 1982.

- 313 Liao, J., L. M. Kistler, C. G. Mouikis, B. Klecker, I. Dandouras, and J.-C. Zhang (2010),  
314 Statistical study of O<sup>+</sup> transport from the cusp to the lobes with Cluster CODIF data, *J.*  
315 *Geophys. Res.*, 115, A00J15, doi:10.1029/2010JA015613.
- 316 Lin, C. C., B. H. Wu, L. C. Lee, and J. K. Chao (2004), Generation of cold O<sup>+</sup> beams observed  
317 in the tail lobe by weak fast shocks in the polar magnetosphere, *J. Geophys. Res.*, 109,  
318 A11214, doi:10.1029/2004JA010422.
- 319 Pitout, F., C. P. Escoubet, B. Klecker, and H. Reme (2006b), Cluster survey of the mid-altitude  
320 cusp: 1. Size, location, and dynamics, *Ann. Geophys.*, 24, 3011–3026.
- 321 Reme, H., et al. (2001), First multispacecraft ion measurements in and near the earth's  
322 magnetosphere with the identical Cluster ion spectrometry (CIS) experiment, *Ann. Geophys.*,  
323 19, 1303–1354.
- 324 Slapak, R., H. Nilsson, M. Waara, G. Stenberg, M. André, and I. A. Barghouthi (2011), O<sup>+</sup>  
325 heating associated with strong wave activity in the high altitude cusp and mantle, *Ann.*  
326 *Geophys.*, 29(5), 931–944.
- 327 Yau, A. W., and M. Andre (1997), Sources of ion outflow in the high latitude ionosphere, *Space*  
328 *Sci. Rev.*, 80, 1–25.
- 329 Yau, A. W., T. Abe, and W. K. Peterson (2007), The polar wind: Recent observations, *J. Atmos.*  
330 *Sol. Terr. Phys.*, 69, 1936–1983, doi:10.1016/j.jastp.2007.08.010.
- 331 Yu, Y., & Ridley, A. J. (2013). Exploring the influence of ionospheric O<sup>+</sup> outflow on  
332 magnetospheric dynamics: Dependence on the source location. *Journal of Geophysical*  
333 *Research: Space Physics*, 118, 1711–1722. <https://doi.org/10.1029/2012JA018411>
- 334 Zeng, C., Wang, C., Duan, S., Dai, L., Fuselier, S. A., Burch, J. L., et al. (2020). Statistical study  
335 of oxygen ions abundance and spatial distribution in the dayside magnetopause boundary

336 layer: MMS observations. *Journal of Geophysical Research: Space Physics*, 125,  
337 e2019JA027323. [https://doi.org/ 10.1029/2019JA027323](https://doi.org/10.1029/2019JA027323)  
338 Zong, Q.-G., X.-Z. Zhou, Y. F. Wang, X. Li, P. Song, D. N. Baker, T. A. Fritz, P. W. Daly, M.  
339 Dunlop, and A. Pedersen (2009), Energetic electron response to ULF waves induced by  
340 interplanetary shocks in the outer radiation belt, *J. Geophys. Res.*, 114, A10204,  
341 doi:10.1029/2009JA014393.

342

343